

## Rational Design of pH-Controlled DNA Strand Displacement

Alessia Amodio,<sup>†,‡,#</sup> Bin Zhao,<sup>§,#</sup> Alessandro Porchetta,<sup>†,#</sup> Andrea Idili,<sup>†</sup> Matteo Castronovo,<sup>‡,||,⊥</sup> Chunhai Fan,<sup>§</sup> and Francesco Ricci<sup>\*,†</sup>

<sup>†</sup>Dipartimento di Scienze e Tecnologie Chimiche, University of Rome, Tor Vergata, Via della Ricerca Scientifica, 00133, Rome, Italy

<sup>‡</sup>School of Nanotechnology, Department of Physics, University of Trieste, Via Valerio 2, 34127 Trieste, Italy

<sup>§</sup>Division of Physical Biology, and Bioimaging Center, Shanghai Synchrotron Radiation Facility, CAS Key Laboratory of Interfacial Physics and Technology, Shanghai Institute of Applied Physics, Chinese Academy of Sciences, Shanghai 201800, China

<sup>||</sup>Department of Medical and Biological Science, University of Udine, Piazzale Kolbe 4, 3310, Udine, Italy

<sup>⊥</sup>Department of Biology, Temple University, 1900 N. 12th Street, Philadelphia, Pennsylvania 19122, United States

### **S** Supporting Information

**ABSTRACT:** Achieving strategies to finely regulate with biological inputs the formation and functionality of DNA-based nanoarchitectures and nanomachines is essential toward a full realization of the potential of DNA nanotechnology. Here we demonstrate an unprecedented, rational approach to achieve control, through a simple change of the solution's pH, over an important class of DNA association-based reactions. To do so we took advantage of the pH dependence of parallel Hoogsteen interactions and rationally designed two triplex-based DNA strand displacement strategies that can be triggered and finely regulated at either basic or acidic pHs. Because pH change represents an important input both in healthy and pathological biological pathways, our findings can have implication for the development of DNA nanostructures whose assembly and functionality can be triggered in the presence of specific biological targets.

DNA nanotechnology uses DNA (or nucleic acids) as a versatile material to rationally engineer tools and molecular devices that can find a multitude of different applications (e.g., in vivo imaging, clinical diagnostics, drug-delivery, etc.).<sup>1</sup> An exciting development of this field, namely structural DNA nanotechnology, is characterized by the use of DNA to build complex nanometer-scale structures, often referred to as DNA origami or DNA tiles.<sup>2</sup> With its simple base-pairing code and its nanoscale dimension, in fact, DNA appears as the perfect building block to assemble and engineer complex molecular architectures with unique accuracy and precision. Similarly, the possibility to quantitatively predict and simulate DNA thermodynamics interactions has allowed to expand the horizons of DNA nanotechnology into the construction of programmable and autonomous DNA-based nanodevices that can be engineered to have different functions.<sup>1–3</sup>

In order to create these complex nanostructures with enough precision and to engineer functional DNA nanodevices it is crucial to strictly control the thermodynamics and the kinetics with which DNA strands interact and hybridize with each other. A beautiful example of such possibility is represented by the

toehold-mediated (or toehold-exchange) DNA strand displacement, a process through which two strands hybridize with each other displacing one (or more) prehybridized strands.<sup>4</sup> Such process, pioneered by Yurke, and later expanded by Zhang, Winfree, and Yurke himself, has been systematically applied to engineer functional DNA nanodevices. These include molecular motors,<sup>3a,5</sup> tweezers,<sup>6,7</sup> autonomous nanomachines,<sup>8,9</sup> circuits,<sup>10</sup> and catalytic amplifiers.<sup>11</sup> Because it can allow a specific kinetic control of several reaction pathways, DNA strand displacement has also found applications in the construction of DNA-based nanostructures and origami.<sup>4b,12</sup>

Despite the advantages represented by strand-displacement to build and engineer complex and functional DNA structures in a controlled way, additional features might help in improving the programmability of this process. For example, we note that, using the conventional approach, once the invading strand (i.e., the strand that activates strand-displacement) is added to the reaction mixture, it is difficult to implement an additional external control to further regulate the process. That is, the strand-displacement reaction performs equally well in different environments (pH, temperature, etc.). While this property can be an advantage for some applications,<sup>13</sup> it can be a limitation for others, as in some cases it could be preferable to exogenously control the entire displacement process. In this context, despite in recent years the DNA strand displacement process has seen a widespread application, only few examples have been reported that allow to activate strand displacement with small molecules<sup>14</sup> (i.e., Hg(II) metal ions and adenosine) or at acidic pHs using i-motif,<sup>15</sup> G-quadruplex,<sup>15</sup> and triplex-forming strands.<sup>16</sup> More recently, light-controlled strand displacement reactions were also demonstrated using photoregulated oligonucleotides.<sup>17</sup>

Motivated by the above arguments, we have rationally designed here two programmable, toehold-based DNA strand displacement strategies that can be triggered and controlled by a simple pH change. We did so by taking advantage of the well-characterized pH sensitivity of the parallel Hoogsteen (T,C)-motif in triplex DNA.<sup>18,19</sup> The sequence-specific formation of a CGC parallel triplet through the formation of Hoogsteen interactions, in fact, requires the protonation of the N3 of

Received: August 19, 2014

Published: November 4, 2014

cytosine in the third strand in order to form (average  $pK_a$  of protonated cytosines in triplex structure is  $\approx 6.5$ ).<sup>20</sup> For this reason, DNA strands containing cytosines can only form a triplex structure at acidic pHs.

More specifically, we designed two complementary strategies, for which DNA-strand displacement is activated either at basic pHs (strategy #1) or at acidic/neutral pHs (strategy #2) (Figure 1a and 1b, respectively). In the first strategy ( $\text{OH}^-$ -activated

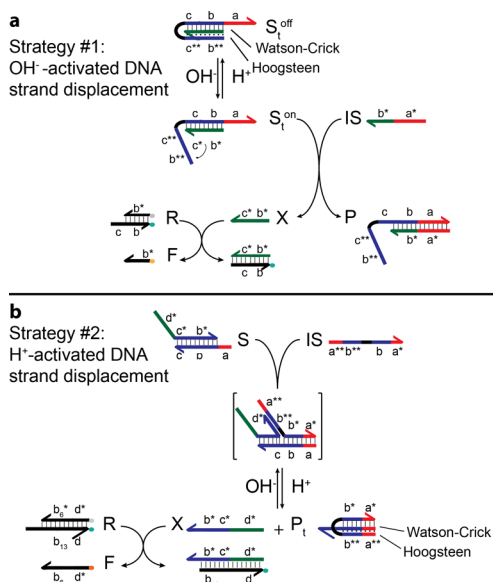


**Figure 1.** The pH-controlled, toehold-based DNA strand displacement strategies. (a) In the first strategy we have designed a DNA strand displacement that is activated at basic pHs ( $\text{OH}^-$ -activated strand displacement). To do this, we have used a clamp-like DNA strand that, under acidic pHs, forms a triplex inactive complex ( $S_t^{\text{off}}$ ) with the strand to be released (X). The additional Hoogsteen interactions in this triplex structures provide an increased stabilization to the complex that prevents strand displacement upon Invading Strand (IS) addition. At basic pHs, the destabilization of the Hoogsteen interactions leads to an active complex ( $S_t^{\text{on}}$ ) characterized by a simple duplex conformation. Because this structure is not stabilized anymore by Hoogsteen interactions, it can undergo displacement through a classic toehold-exchange mechanism. (b) In the second strategy we designed a toehold-based DNA strand displacement process that is activated at acidic/neutral pHs ( $\text{H}^+$ -activated strand displacement). To do this, we have designed an IS comprised of a triplex-competent DNA sequence that can bind through a clamp-like mechanism a strand in the complex S. Under basic conditions, this IS can only form Watson–Crick interactions and, due to the content and length of the toehold-binding ( $a^*$ ) and invading ( $b^*$ ) portion, strand displacement process is unfavored. In contrast, at acidic pHs, triplex formation through Hoogsteen interactions provides an additional energetic contribution that allows strand displacement to occur. In this study the progress of strand displacement is always followed using an optically labeled reporter complex (R) that stoichiometrically reacts with the released strand (X) to produce an unquenched fluorophore-labeled single strand DNA molecule (F). We note that the reaction between the reporter complex (R) and the released strand (X) is not sensitive to pH in the pH range we have investigated (Figures S11 and S12) and does not directly take part to the strand displacement reaction.<sup>4</sup> In this paper, domains are represented by letters. Starred letters (\*) represent domains complementary to the domains denoted by unstarred letters and forming classic Watson–Crick base pairings. Double starred letters (\*\*) represent triplex-forming domains that form Hoogsteen interactions with duplex formed by the domains denoted by starred (\*) and unstarred letters.

strand displacement), a clamp-like, triplex-forming DNA prevents strand displacement at acidic pHs (conditions at which triplex formation is favored) (Figure 1a), while at basic pHs (when Hoogsteen interactions are destabilized) a classic strand-displacement reaction is observed. In the second strategy ( $\text{H}^+$ -activated strand displacement), in contrast, the invading strand (IS) contains a clamp-like triplex forming portion. Only under pH conditions (acid/neutral) at which Hoogsteen interactions can form and we observe the strand displacement process (Figure 1b).

Both strategies rely on the use of pH-dependent clamp-like conformational switches (Figure 1) that lead to triplex formation.<sup>18</sup> In the first strategy triplex formation is utilized to lock the strand that would be otherwise released in the presence of the IS. In the second strategy, in contrast, clamp-like triplex formation triggers strand displacement. As a first characterization of both strategies, we have thus studied the pH-dependent stability of the corresponding clamp-like triplex complexes. To do this we have initially studied the pH-dependent stability of the triplex complex ( $S_t^{\text{off}}$ ) in strategy #1 (Figure 2a). More

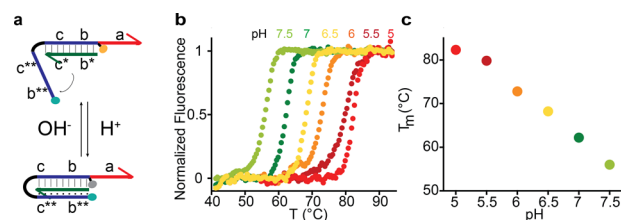


**Figure 2.** The pH-dependent clamp-like triplex DNA formation. (a) Folding/unfolding of the triplex complex of strategy #1 (see Figure 1a) is monitored here through a pH-insensitive FRET pair located in an internal position (Cy3) and at the 5'-end (Cy5) of the clamp-like strand. (b) Shown are the melting denaturation curves of the complex  $S_t$  (20 nM) obtained at different pH values in a 0.01 M Tris buffer solution +0.01 M MgCl<sub>2</sub>. (c) At a pH at which triplex formation is favored (pH = 5), the melting temperature of the complex is 82.3 °C. As the acidity of the solution is progressively reduced to reach pH 7.5, at which triplex formation is unfavored, the complex is progressively destabilized until it reaches a melting temperature of 56.0 °C.

specifically, we have used a dual labeled clamp-like triplex forming strand, and after hybridization to a target DNA oligo, we have performed thermal denaturation of the so-formed complex at different pHs (Figure 2b). As expected, under acidic pHs, a condition at which triplex formation is favored,<sup>18</sup> the overall stability of the complex is improved. For example, at a pH low enough to allow triplex formation (pH = 5), the denaturation of the complex occurs at very high temperatures (i.e.,  $T_m = 82.3$  °C). In contrast, under pH values at which triplex formation is unfavored (pH = 7.5), the denaturation of the complex occurs at a much lower temperature ( $T_m = 56.0$  °C) (Figure 2c). A similar pH dependence has been observed with the clamp-like strands of strategy #2 (Figure S13). We also note that at acidic pH the possible alternative i-motif<sup>21</sup> that the triplex-forming strand (in Figure 1:  $c^{**}b^{**}$ ) could form does not affect the pH dependence of our system. These results demonstrate that the clamp-like triplex formation based on Hoogsteen interactions offers highly efficient and tunable pH regulation, which could be suitable toward the realization of pH-dependent DNA-based molecular devices.

Triplex formation in both the strategies we present here allows to rationally control the displacement process by simply changing the solution's pH. For example, for strategy #1

(OH<sup>-</sup>-activated strand displacement), at pH 8 (a pH at which triplex formation is unfavored), strand displacement proceeds with a fast kinetic upon IS addition (Figure 3a, top). At pH 5, in contrast, which is acidic enough for the clamp-like strand to form a triplex, inactive complex ( $S_t^{\text{off}}$ ) (see Figure 2a), the addition of the IS does not result in any significant signal change (Figure 3a, bottom), suggesting that no displacement occurs. Such pH-dependent strand displacement process is observed over a wide range of IS concentrations. A conventional strand displacement

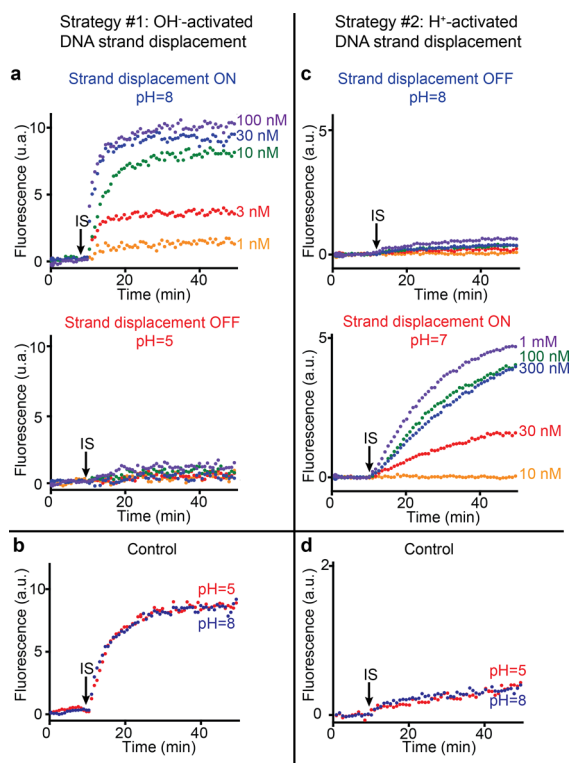


**Figure 3.** OH<sup>-</sup>- and H<sup>+</sup>-activated toehold-based DNA strand displacement. (Left) In the first strategy we dissected here (OH<sup>-</sup>-activated strand displacement), strand displacement is only observed at basic pHs (a, top), while under acidic pHs (a, bottom) triplex formation leads to a very stable complex ( $S_t^{\text{off}}$ , Figure 1a) that prevents strand displacement. Such pH dependence is observed over a wide range of IS concentrations (from 1 to 100 nM). A control toehold-based DNA strand displacement that uses the same sequences except for the fact that it lacks the terminal triplex-forming portion ( $b^{**}$  and  $c^{**}$ ) is, as expected, independent of pH (b). Here, we used an IS with a toehold-binding portion ( $a^*$  in Figure 1a) of 15 bases and an invading portion ( $b^*$  in Figure 1a) of 10 bases. Electrophoresis experiments (PAGE) confirm such pH dependency (Figure S19). (Right) In the second strategy we have used here (H<sup>+</sup>-activated strand displacement) the addition of the IS under basic conditions (pH 8) does not result in any significant strand displacement reaction (c, top). Strand displacement reaction is triggered at acidic pHs, due to the formation of a triplex complex (c, bottom). Also in this case, such pH dependence is observed over a wide range of IS concentrations (from 10 nM to 1  $\mu$ M). A control IS with the same toehold-binding and invading domains as the one used above but lacking the triplex forming portion ( $a^{**}$  and  $b^{**}$ ) does not lead to any displacement reaction over the entire pH range we have investigated (d). Fluorescence signals shown here have been subtracted from the background signal. Strand displacement in both these strategies is followed by fluorescence measurements obtained in a solution of complex S (10 nM) in the presence of reporter R (30 nM) after the addition of the IS at a concentration of 30 nM in a 0.01 M Tris buffer + 0.01 M MgCl<sub>2</sub> at 25 °C.

toehold-exchange process (thus based on a complex that cannot form a triplex structure) is independent of pH and occurs with very similar kinetics in the entire pH range we have investigated (Figure 3b) and over a wide range of IS concentrations (Figure S14).<sup>4c</sup> Of note, this duplex-only control complex (used here for a comparison) has the same sequence of that used in the OH<sup>-</sup>-activated strand displacement process except that it lacks the domains  $b^{**}$  and  $c^{**}$ , i.e., the portions able to form the triplex (see Figure 1a and Materials).

Because triplex stability can be tuned at different pHs (see Figure 2), we can achieve a gradual inhibition/activation of the strand displacement process by gradually changing the solution's pH (Figure S15). As expected, intermediate kinetics are observed under pH conditions at which triplex/duplex equilibrium is more balanced (around pH 7). Again, such tunable behavior is observed over a wide concentration range of IS (i.e., from 1 to 100 nM) (Figure S16). Different degree of inhibition can also be achieved varying the IS length (Figures S17 and S18). For example, by changing the pH of the solution from pH 8 to 5 we can observe only a partial inhibition of the displacement reaction using an IS containing an invading domain of 12 bases (Figure S17). With the same pH change we observe a complete inhibition of the displacement process when we use shorter invading domains (i.e., 10 and 8 bases) (Figure S17). A similar trend is observed at different pH values and with different concentrations of IS (Figure S18).

In the second strategy (H<sup>+</sup>-activated DNA strand displacement) we present here, pH-dependent triplex formation triggers strand displacement. Of note, in this case, contrarily to the first strategy described above, the triplex forming portion is within the IS (Figure 1b). At pH 8 (triplex destabilizing condition), the addition of the IS does not result in any significant fluorescence signal increase (Figure 3c, top). In contrast, at pH 7 (a pH low enough to form already a triplex complex), the addition of the IS successfully leads to the strand displacement reaction (Figure 3c, bottom). In this H<sup>+</sup>-activated strategy, a pH change of just one unit (from pH 8 to 7) will be sufficient to activate the strand displacement process. Similarly to what we have achieved with the OH<sup>-</sup>-activated strategy, also in this case the pH-dependent behavior is observed over a wide range of IS concentration (from 30 nM to 1  $\mu$ M, see Figure S110). A control experiment obtained using an IS with the same sequence used above except that it lacks the domains  $a^{**}$  and  $b^{**}$ , i.e., the portion necessary to form the triplex (see Figure 1b and Materials) shows that the displacement process is independent of pH, as expected. More specifically, we did not observe any significant displacement signal over the entire pH range investigated (from 5 to 8) and over the same IS concentration range (from 30 nM to 1  $\mu$ M) (Figures 3d and S111).

Both the strategies we have dissected here allow an external control over the strand displacement process. We further demonstrate this by adding the IS under initial inhibiting conditions (Figure 4) for both strategies. The addition of the IS under these conditions does not lead to any significant strand displacement (Figure 4, red lines). Upon addition of either OH<sup>-</sup> (Figure 4a) or H<sup>+</sup> (Figure 4b), we were able to activate both processes, and we observed an immediate increase of the fluorescence signals associated with the strand displacement reactions (Figure 4, blue curves). A similar feature has been observed over a wide IS concentration range (Figure S112).

Here we have rationally designed triplex-based DNA strand displacement reactions that, in contrast to previous pH-controlled examples, can be triggered/activated at both basic

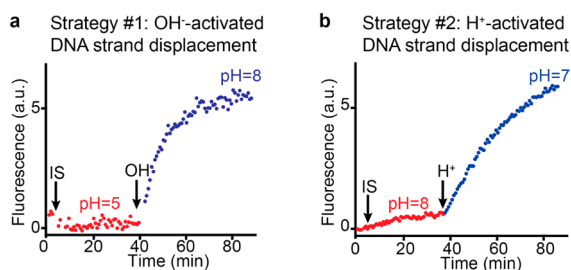


**Figure 4.** Toehold-based DNA strand displacement in the triplex-DNA based strategies we propose here can be triggered by changing the solution's pH. Under inhibiting conditions the addition of the IS does not result in any displacement reaction (red lines). Upon addition of (a)  $\text{Na}_2\text{CO}_3$  (to reach a pH of 8) or (b)  $\text{NaH}_2\text{PO}_4$  (to reach a neutral pH) strand displacement is triggered, and we observe a fast signal increase (blue lines). Experiments were performed in a 0.01 M Tris buffer +0.01 M  $\text{MgCl}_2$ , at 25 °C.

and acidic pHs. We did so by taking advantage of the pH dependence of parallel Hoogsteen interactions and designing clamp-like DNA strands that, by forming a triplex complex under acidic pHs, can trigger or inhibit strand displacement reactions.

We note that alternative DNA or RNA base pairings (Hoogsteen, sugar edges, etc.) and secondary DNA structures (i-motif, G-quadruplex, etc.) are likely more amenable to exogenous control (pH,  $\text{Mg}^{2+}$ , etc.) than the classic Watson–Crick base pairings. This might open the future to new and exciting possibilities in the field of functional DNA nanotechnology. Compared with other pH-dependent DNA secondary structures (e.g., the i-motif),<sup>21,22</sup> the use of triplex DNA might allow a better control and a tunable pH-dependency over a wide pH range.<sup>18b</sup>

The possibility to activate/inhibit the toehold-exchange DNA strand displacement process through a simple change of the solution's pH appears particularly interesting for several reasons. Since strand displacement has been used to assemble dynamic and static DNA-based nanostructures<sup>4b,12</sup> the strategies presented in this work could be adopted to introduce additional control over the formation and functionality of similar DNA nanoarchitectures. For example, our approach would permit in principle to regulate DNA-based origami formation or DNA-based nanodevices' activity exclusively through pH changes. In addition, since pH dysregulation is often associated with different diseases (e.g., many cancers are characterized by an inverted pH gradient between the inside and the outside of cells),<sup>23</sup> it could be useful to activate the functionality of drug-releasing DNA-based nanomachines only at specific pH values.

## ■ ASSOCIATED CONTENT

### Supporting Information

Supporting methods and figures. This material is available free of charge via the Internet at <http://pubs.acs.org>.

## ■ AUTHOR INFORMATION

### Corresponding Author

francesco.ricci@uniroma2.it

### Author Contributions

<sup>#</sup>These authors contributed equally.

### Notes

The authors declare no competing financial interest.

## ■ ACKNOWLEDGMENTS

This work was supported by Associazione Italiana per la Ricerca sul Cancro, AIRC (project n. 14420) (F.R.), by the European Research Council, ERC (project n.336493) (F.R.), (project no. 269051-Monalisa's Quidproquo) (A.A., M.C.), by the Int. Research Staff Exchange Scheme (IRSES) and by the Nando Peretti Foundation (F.R.).

## ■ REFERENCES

- (1) (a) Krishnan, Y.; Bathe, M. *Synth. Cell Biol.* **2012**, *22*, 624. (b) Lu, C. H.; Willner, B.; Willner, I. *ACS Nano* **2013**, *7*, 8320.
- (2) (a) Douglas, S. M.; Bachelet, I.; Church, G. M. *Science* **2012**, *335*, 831. (b) Winfree, E.; Liu, F.; Wenzler, L. A.; Seeman, N. C. *Nature* **1998**, *394*, 539. (c) Rothmund, P. W. K. *Nature* **2006**, *440*, 297.
- (3) (a) Turberfield, A. J.; Mitchell, J. C.; Yurke, B.; Mills, A. P., Jr.; Blakey, M. I.; Simmel, F. C. *Phys. Rev. Lett.* **2003**, *90*, 118102/1. (b) Bath, J.; Turberfield, A. J. *Nat. Nanotechnol.* **2007**, *2*, 275. (c) Mao, C. *Nat. Nanotechnol.* **2008**, *3*, 75. (d) Krishnan, Y.; Simmel, F. C. *Angew. Chem., Int. Ed.* **2011**, *50*, 3124.
- (4) (a) Seelig, G.; Soloveichik, D.; Zhang, D. Y.; Winfree, E. *Science* **2006**, *314*, 1585. (b) Zhang, D. Y.; Seelig, G. *Nat. Chem.* **2011**, *3*, 103. (c) Zhang, D. Y.; Winfree, E. *J. Am. Chem. Soc.* **2009**, *131*, 17303.
- (5) Wickham, S. F. J.; Bath, J.; Katsuda, Y.; Endo, M.; Hidaka, K.; Sugiyama, H.; Turberfield, A. J. *Nat. Nanotechnol.* **2012**, *7*, 169.
- (6) Han, X.; Zhou, Z.; Yang, F.; Deng, Z. *J. Am. Chem. Soc.* **2008**, *130*, 14414.
- (7) Liu, M.; Fu, J.; Hejesen, C.; Yang, Y.; Woodbury, N. W.; Gothelf, K.; Liu, Y.; Yan, H. *Nat. Commun.* **2013**, *4*, 2127.
- (8) Yang, Y.; Liu, G.; Liu, H.; Li, D.; Fan, C.; Liu, D. *Nano Lett.* **2010**, *10*, 1393.
- (9) Zhu, C.; Wen, Y.; Li, D.; Wang, L.; Song, S.; Fan, C.; Willner, I. *Chem.–Eur. J.* **2009**, *15*, 11898.
- (10) (a) Elbaz, J.; Lioubashevski, O.; Wang, F.; Remacle, F.; Levine, R. D.; Willner, I. *Nat. Nanotechnol.* **2010**, *5*, 417. (b) Genot, A. J.; Bath, J.; Turberfield, A. J. *J. Am. Chem. Soc.* **2011**, *133*, 20080.
- (11) Sun, Y.-H.; Kong, R.-M.; Lu, D.-Q.; Zhang, X.-B.; Meng, H.-M.; Tan, W.; Shen, G.-L.; Yu, R.-Q. *Chem. Commun.* **2011**, *47*, 3840.
- (12) (a) Chen, H.; Weng, T.-W.; Riccitelli, M. M.; Cui, Y.; Irudayaraj, J.; Choi, J. H. *J. Am. Chem. Soc.* **2014**, *136*, 6995. (b) Wang, F.; Lu, C.-H.; Willner, I. *Chem. Rev.* **2014**, *114*, 2881. (c) Baker, B. A.; Mahmoudabadi, G.; Milam, V. T. *Soft Matter* **2013**, *9*, 11160.
- (13) (a) Zhang, D. Y.; Chen, S. X.; Yin, P. *Nat. Chem.* **2012**, *4*, 208.
- (14) (a) Xu, X.; Yang, X. *Chem. Commun.* **2014**, *50*, 805. (b) Ding, W.; Deng, W.; Zhu, H.; Liang, H. *Chem. Commun.* **2013**, *49*, 9953.
- (15) Tang, W.; Wang, H.; Wang, D.; Zhao, Y.; Li, N.; Liu, F. *J. Am. Chem. Soc.* **2013**, *135*, 13628.
- (16) Liu, Z.; Mao, C. *Chem. Commun.* **2014**, *50*, 8239.
- (17) (a) Jester, S.-S.; Famulok, M. *Acc. Chem. Res.* **2014**, *47*, 1700. (b) Kamiya, Y.; Asanuma, H. *Acc. Chem. Res.* **2014**, *47*, 1663. (c) Lohmann, F.; Ackermann, D.; Famulok, M. *J. Am. Chem. Soc.* **2012**, *134*, 11884. (d) Lohmann, F.; Weigandt, J.; Valero, J.; Famulok, M. *Angew. Chem., Int. Ed.* **2014**, *126*, 10540.
- (18) (a) Idili, A.; Plaxco, K. W.; Vallée-Bélisle, A.; Ricci, F. *ACS Nano* **2013**, *7*, 10863. (b) Idili, A.; Vallée-Bélisle, A.; Ricci, F. *J. Am. Chem. Soc.* **2014**, *136*, 5836.
- (19) Ohmichi, T.; Kawamoto, Y.; Wu, P.; Miyoshi, D.; Karimata, H.; Sugimoto, N. *Biochemistry* **2005**, *44*, 7125.
- (20) Soto, A. M.; Loo, J.; Marky, L. A. *J. Am. Chem. Soc.* **2002**, *124*, 14355.
- (21) Li, T.; Ackermann, D.; Hall, A. M.; Famulok, M. *J. Am. Chem. Soc.* **2012**, *134*, 3508. Li, T.; Famulok, M. *J. Am. Chem. Soc.* **2013**, *135*, 1593.
- (22) Modi, S.; Nizak, C.; Surana, S.; Halder, S.; Krishnan, Y. *Nat. Nanotechnol.* **2013**, *8*, 459.
- (23) Webb, B. A.; Chimenti, M.; Jacobson, M. P.; Barber, D. L. *Nat Rev Cancer* **2011**, *11*, 671.